ISSN 1062-8738, Bulletin of the Russian Academy of Sciences. Physics, 2012, Vol. 76, No. 9, pp. 995–998. © Allerton Press, Inc., 2012.
Original Russian Text © V.V. Privezentsev, M.V. Chukichev, R.V. Mironov, Yu.V. Krivenkov, 2012, published in Izvestiya Rossiiskoi Akademii Nauk. Seriya Fizicheskaya, 2012, Vol. 76, No. 9, pp. 1107–1110.

Investigating the Optical Properties of a Near-Surface Layer in Silicon Implanted by Zinc after Thermal Annealing

V. V. Privezentsev[a], M. V. Chukichev[b], R. V. Mironov[c], and Yu. V. Krivenkov[d]

[a] *Physicotechnical Institute, Russian Academy of Sciences, Moscow, 117218 Russia*
[b] *Faculty of Physics, Moscow State University, Moscow, 119991 Russia*
[c] *Fiber Optics Research Center, Russian Academy of Sciences, Moscow, 119333 Russia*
[d] *Molecular Electronics Research Institute and Micron Factory, Moscow, 124460 Russia*
e-mail: privezentsev@ftan.ru

Abstract—Changes in the optical properties of a Si layer broken as a result of implantation by Zn ions are investigated during thermal annealing. The investigations are performed by Raman scattering (RS), ellipsometry, and cathodoluminescence (CL). The implanted samples show a broken area with a thickness of about 60 nm with partial amorphization. Thermal treatment at 400°C results in the partial annealing of a radiation point defect while reducing the thickness of the broken layer to 40 nm. The broken layer was completely restored after high-temperature annealing at 700°C.

DOI: 10.3103/S1062873812090213

INTRODUCTION

The use of metallic and oxide nanoclusters (NCs) in various matrices, particularly on silicon substrates, is now assuming great importance for optoelectronics [1]. NCs of ZnO play a special role among such materials, since ZnO is a direct-bandgap material with a bandgap of 3.37 eV and has great electron and hole binding energy in excitons of 60 meV. Such NCs can be widely applied in such modern optoelectronic devices as lasers [2], solar cells [3], and electroluminescent displays [4]. NCs of ZnO can be formed by thermal treatment in an inert oxidizing medium of Si with Zn precipitates. Ionic implantation allows us to obtain Zn concentrations much higher than its limiting equilibrium solubility in Si, which is 6×10^{16} cm^{-3} [5] at a diffusion temperature of 1250°C. This work presents the findings from our investigation of the effect of thermal treatment on the optical properties of a near-surface layer of Si implanted with Zn. The investigations were conducted by means of Raman scattering (RS), ellipsometry, and cathodoluminescence (CL).

EXPERIMENTAL

Plates of single-crystal CZ-*n*-Si (100), 350 μm thick with electron concentrations $n_0 = 5 \times 10^{15}$ cm^{-3}, were implanted by $^{64}Zn^+$ with dose $D = 2 \times 10^{14}$ cm^{-2} and energy $E = 100$ keV. After implantation, the plates were annealed in N_2 at $t = 400$°C for 60 min and then in Ar at $t = 700$°C for 20 min. The CL spectra were recorded at temperature $T = 80$ K on a pulsed gun with an accelerating voltage of 20 kV and a pulse duration of 0.2 μs, a relative pulse duration of 2.5×10^4, and a pulse current of 250 mA. The RS spectra were measured on a T 64000 device (Jobin Yvon). The ellipsometry spectra were investigated using an Ellips-1891 spectral device (Institute of Semiconductor Physics, Siberian Branch,e Russian Academy of Science) at wavelength $\lambda = 5145$ Å.

RESULTS AND DISCUSSION

Figure 1 presents the RS spectra for the investigated samples: 1 implanted silicon; 2 annealed at 400°C; 3 annealed at 400°C + 700°C; 4 initial KEF 4.5 silicon; 5 polycrystalline natural silicon (k-Si). The spectra are separated along the vertical for the sake of clarity. The RS spectrum for the sample after implantation is similar to the amorphous silicon spectrum since we can discern the bands with maxima in the range of 150, 290, 390, and 470 cm^{-1} that belong to amorphous Si [6]. The narrow peak at around 520 cm^{-1} belongs to the nonamorphized areas of the crystalline silicon substrate. The growth of this peak after the thermal treatment at 400°C verifies the partial annealing of radiation defects. The RS spectrum after annealing at 700°C closely matches the initial silicon spectra, indicating almost complete recrystallization of the layer that was broken as a result of implantation.

The wide spectrum of the sample after implantation is similar to the spectrum of amorphous silicon (Fig. 2) because it has clear wide bands with maxima in the range of 290, 390, 470 cm^{-1} and a low-frequency band in the range of 100 to 200 cm^{-1}. These bands can be compared to the RS spectrum of amor-

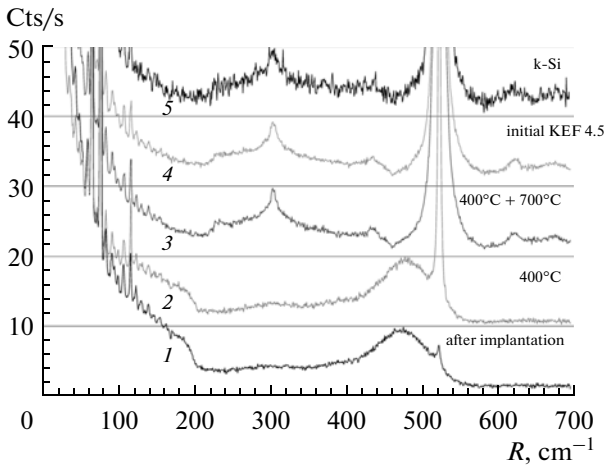

Fig. 1. RS spectra of investigated samples: (1) implanted silicon; (2) annealed at 400°C; (3) annealed at 400°C + 700°C; (4) initial KEF 4.5 silicon; (5) polycrystalline natural silicon (k-Si).

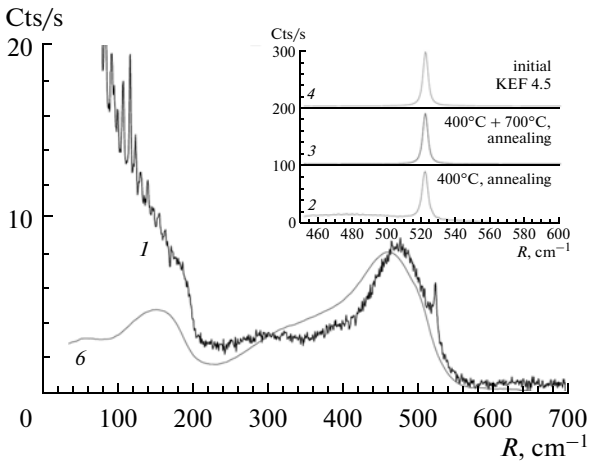

Fig. 2. RS spectra of investigated samples: (1) implanted silicon; (6) amorphous silicon. The insert shows the RS spectra of investigated samples in the area of the main peak of the Si–Si bond at a wavelength of 521 cm^{-1}: (2) annealed at 400°C; (3) annealed at 400°C + 700°C; (4) initial KEF 4.5 silicon.

phous silicon. The slight observable difference in the spectra can be explained by the degree of amorphization and the technique used in making the investigated samples. The narrow low-intensity peak at 521 cm^{-1} could belong to nonamorphized (crystalline) areas remaining in the investigated sample after processing.

As is evident from Fig. 1, annealing at 400°C results in the partial (gradual) crystallization of the sample; annealing at 700°C results in the complete crystallization of the sample because, as is evident from Fig. 1, the RS spectrum of such an annealed sample is identical to the initial silicon spectrum. The RS spectrum of the initial silicon sample is identical to the spectrum of polycrystalline natural silicon, shown in Fig. 1, since the intense peak at 521 cm^{-1} belongs to crystalline natural silicon (Fig. 2, insert).

In ellipsometry, a linearly-polarized wave falls onto the investigated sample and becomes elliptically polarized after reflecting from the surface under investigation. The parameters of the polarization ellipse (i.e., the orientation of its axes and eccentricity) are determined by the optical properties of the reflecting surface's structure and the light's angle of incidence. Experimental measurements were made for the ratio of complex reflection factors for two types of light wave polarization: in the incident plane (p) and perpendicular to it (s). This ratio is expressed through the ellipsometric parameters ψ (amplitude) and Δ (phase), which characterize the relative change of amplitudes for the p- and s polarizations and the phase shift between them [7]:

$$\tan\Psi \exp i\Delta = \frac{R_p}{R_s}, \qquad (1)$$

λ is the radiation wavelength, and d is the jth layer thickness.

$$R_{p,s}^{j+1} = \frac{r_{p,s}^{j+1} + R_{p,s}^{j} \exp(-i2\beta_j)}{1 + r_{p,s}^{j+1} R_{p,s}^{j} \exp(-i2\beta_j)}, \qquad (2)$$

where $R_{p,s}^{j+1}$ are the complex reflection factors for the p- and s polarizations at the boundary of the jth and $(j+1)$th layers, which are expressed recurrently through $R_{p,s}^{j}$, the r_p and r_s Fresnel coefficients at the boundary of the jth and $(j+1)$th layers are

$$r_p^{j+1} = \frac{N^{j+1}\cos(\varphi_j) - N^j \cos(\varphi_{j+1})}{N^{j+1}\cos(\varphi_j) + N^j \cos(\varphi_{j+1})},$$
$$r_s^{j+1} = \frac{N^{j}\cos(\varphi_j) - N^{j+1} \cos(\varphi_{j+1})}{N^{j}\cos(\varphi_j) + N^{j+1} \cos(\varphi_{j+1})}, \qquad (3)$$

where N is the complex refraction index of the corresponding layer, $\cos(\varphi_j)$ is the complex cosines of the angle of reflection for the jth layer, and the parameter β is

$$\beta_j = \frac{2\pi d^j N^j \cos(\varphi_j)}{\lambda}, \qquad (4)$$

where the $(J+1)$th layer is placed over the Jth layer, and then over the $(J-1)$th layer, λ is the radiation wavelength, and d is the jth layer thickness.

From Eq. (1), we can determine any two parameters of the model describing the reflection factors R_p and R_s, depending on the optical properties of the structure under investigation and the light's angle of incident and wavelength.

Experimental measurements were made for the Ψ and Δ spectra during optical wavelength scanning (spectral ellipsometry) in the range of 250 to 900 nm for all three samples, i.e., samples after implantation

(no. 1), preliminary annealing (no. 2), and high-temperature annealing (no. 3).

The ellipsometry spectra are presented in Fig. 3. Their interpretation required us to choose a physical model for describing the actual structure formed as a result of implantation and annealings. The physical model was a four-layer structure consisting of a film of SiO_2, a broken silicon layer, and an unbroken silicon substrate, with the structure kept in air (there were three interfaces). Our model of the investigated structure assumes that $N = n - i \times k$, where n is the refraction index and k is the absorption factor ($i = \sqrt{-1}$) for each wavelength and for all four layers (substrate, broken layer, oxide, air). The sought quantities are the thicknesses of layers d_{am} and d_{SiO_2}. We then performed mathematical simulations for the right part of Eq. (1), based on the set of equations (2)–(4) describing the selected physical model, in which the optical properties of the broken layer are considered to be analogous to the properties of amorphous silicon. The set of equations for the selected model was then solved numerically, and the sought parameters of the selected physical model were then determined, i.e., the thicknesses of the broken layer and the oxide film.

We succeeded in establishing the following:

(i) Immediately after implantation, the calculated and experimental dependences agree fairly well quantitatively for wavelengths of 650–850 nm. It was determined that the thickness of the SiO_2 film was 2.5 nm, and that of the broken silicon layer was 60 nm.

(ii) After annealing at 400°C in a wavelength range of 650–850 nm, the calculated and experimental dependences agree only qualitatively in the nature of the dependence; at the same time, it was determined that the thickness of the SiO_2 film was invariable, and the thickness of the broken layer was reduced to 40 nm.

(iii) After annealing at 700°C the calculated and experimental dependences agreed with a rather high degree of accuracy; it was found that there was no broken layer and there was only a SiO_2 film with a thickness of 3.5 nm.

The optical properties of the broken layer were taken from the table for amorphous silicon contained in the software of the spectral ellipsometer. It is evident that the actual broken layer was not quite the equivalent of amorphous silicon. This could explain the good agreement between the model and the experimental ellipsometry spectra when there is no broken layer after annealing at 700°C, the semiquantitative agreement of spectra immediately after implantation, and their qualitative similarity upon annealing at 400°C, when the actual sample is apparently described by a more complex structure.

Figure 4 presents the CL spectra. The spectrum of the sample after implantation (1) has a wide maximum at wavelength $\lambda = 4600$ Å that is caused by defects. After annealing at 400°C, the CL signal produced by these defects diminishes, and the signal maximum moves to

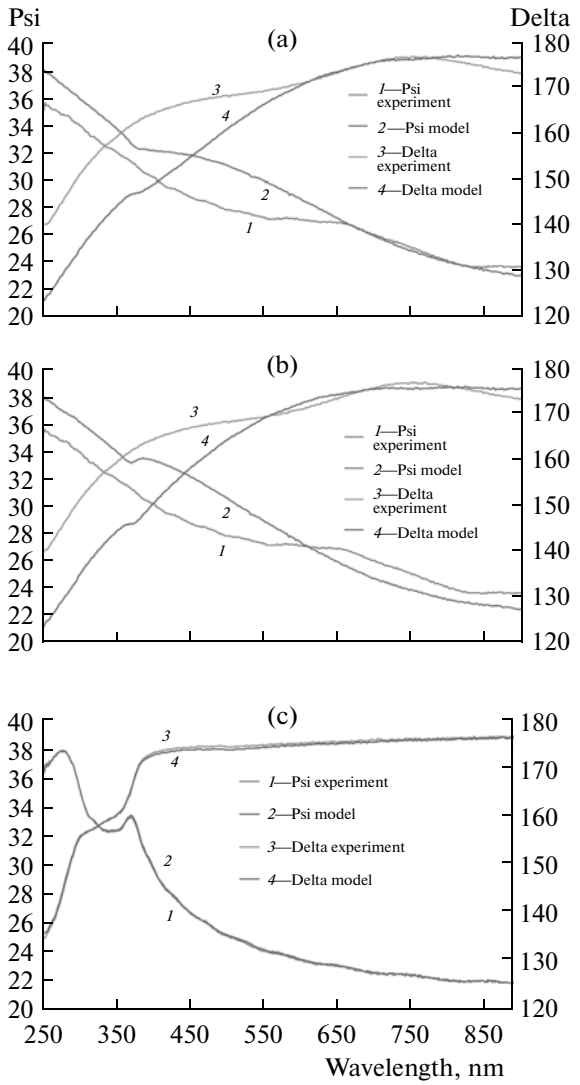

Fig. 3. Ellipsometry spectra: (a) implanted silicon; (b) annealed at 400°C; (c) annealed at 400°C + 700°C.

$\lambda = 5000$ Å. After annealing at 700°C, the CL spectrum exhibits a noticeable peak at wavelength $\lambda = 4500$–5000 Å against the background of the reduced spread maximum in the range of $\lambda = 4000$ Å. This peak could be due to the emergence of a new phase, ZnO. Zinc oxide usually exhibits a spread luminescence peak in the range of 450 to 650 nm. This peak is associated with the deep doped levels caused by the nonstoichiometry of the sample, i.e., internodal zinc atoms and oxygen vacancies. It could be due to intracenter transitions in the atoms of copper which is often present in zinc oxide as an uncontrolled technological impurity.

It was found by X-ray phase analysis that the silicon implanted by zinc ions contains inclusions of metallic zinc. As the annealing temperature rises, the metallic zinc phase was converted into its oxide phase, i.e., into the form of zinc oxide (ZnO). The presence of zinc

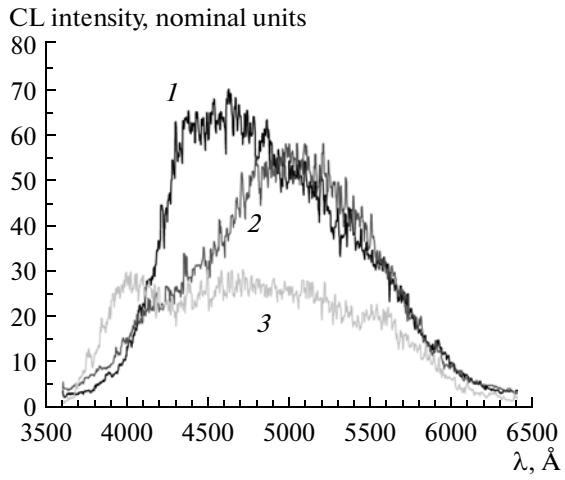

Fig. 4. CL spectra: (1) implanted silicon; (2) annealed at 400°C; (3) annealed at 400°C + 700°C.

silicide in the $ZnSiO_3$ form also is possible in zinc-implanted and annealed silicon layers.

CONCLUSIONS

It follows from the RS and CL spectra that implantation results in the formation of a broken area with amorphization. From the ellipsometry spectra, we can see that the investigated sample after implantation is essentially a three-layered structure consisting of a single crystal substrate, a broken near-surface silicon layer with a thickness of ~60 nm, and a near-surface silicon oxide layer 3.5 nm thick.

Thermal treatment at 400°C for 60 min results in the partial annealing of radiation defects and the restoration of the sample's crystalline structure. The thickness of the broken silicon layer was reduced to 40 nm, and the thickness of the oxide film was invariable. The surface silicon layer that was broken due to implantation completely had its crystalline structure restored after annealing at 700°C for 20 min. The thickness of the surface SiO_2 film was 3.5 nm. It follows from the CL spectra that annealing at 700°C forms ZnO particles.

REFERENCES

1. *Nanoclusters and Nanocrystals*, Singh Nalwa, H., Ed., Hitachi, 2003.
2. Chu, S., Olmedo, M., Yang, Zh., et al., *Appl. Phys. Lett.*, 2008, vol. 93, p. 181106.
3. Jiang, C.Y., Sun, X.W., Lo, G.Q., et al., *Appl. Phys. Lett.*, 2007, vol. 90, p. 263501.
4. Li, C., Yang, Y., Sun, X.W., et al., *Nanotecnology*, 2007, vol. 18, p. 135604.
5. Milnes, A.G., *Deep Impurities in Semiconductors*, New York: Wiley, 1973; Moscow: Mir, 1977.
6. Bagratashvili, V.N., et al., *Sverkhkritich. Flyuidy: Teor. Prakt.*, 2010, no. 2, p. 79.
7. Shvets, V.A., Spesivtsev, E.V., Rykhlitskii, S.V., and Mikhailov, N.N., *Ross. Nanotekhnol.*, 2009, vol. 4, nos. 3–4, p. 72.
8. Azzam, R.M.A. and Bashara, N.M., *Ellipsometry and Polarized Light*, Amsterdam: North Holland, 1977; Moscow: Mir, 1981.